AJNR

Magnetization Transfer Ratio Values and Proton MR Spectroscopy of Normal-appearing Cerebral White Matter in Patients with Liver Cirrhosis

Alex Rovira, Elisenda Grivé, Salvador Pedraza, Antoni Rovira and Juli Alonso

AJNR Am J Neuroradiol 2001, 22 (6) 1137-1142
http://www.ajnr.org/content/22/6/1137

AJNR Am J Neuroradiol 22:1137–1142, June/July 2001

Magnetization Transfer Ratio Values and Proton MR Spectroscopy of Normal-appearing Cerebral White Matter in Patients with Liver Cirrhosis

Alex Rovira, Elisenda Grivé, Salvador Pedraza, Antoni Rovira, and Juli Alonso

BACKGROUND AND PURPOSE: **Hepatic encephalopathy in cirrhotic patients may be the clinical manifestation of disturbed cerebral cell volume homeostasis. The aim of this study was to investigate the presence of significant changes in magnetization transfer ratio (MTR) values, which could reflect an increase in free water within the brain of patients with liver cirrhosis, and to correlate these findings with minimal hepatic encephalopathy and proton MR spectroscopy (^{1}H-MRS) abnormalities.**

METHODS: **Twenty-four patients with liver cirrhosis and eight healthy control volunteers were included in the study. MR imaging studies included conventional T1- and T2-weighted imaging, ^{1}H-MRS, and magnetization transfer imaging. MTR and ^{1}H-MRS values were obtained from normal-appearing white matter and were correlated with each other and with the presence of minimal hepatic encephalopathy.**

RESULTS: **^{1}H-MRS showed a decrease in choline and *myo*-inositol and an increase in glutamine + glutamate with respect to creatine + phosphocreatine. MTR values were significantly decreased in cirrhotic patients when compared with healthy control volunteers, although this decrease was not significantly higher in the patients with minimal hepatic encephalopathy. The decreases in MTR values correlated with increases in glutamine + glutamate.**

CONCLUSION: **The MTR decrease in patients with liver cirrhosis may be caused by low-grade astrocytic swelling produced as a response to the osmotic stress occurring in these patients. However, in this cross-sectional study, we did not find a correlation between MTR decrease and the presence of minimal hepatic encephalopathy, probably because of limitations in MTR quantification techniques.**

MR imaging and proton MR spectroscopy (^{1}H-MRS) brain abnormalities have been described in association with chronic liver disease (1, 2). Results from experimental studies indicate that a widespread metabolic alteration in the brain, which seems to be related to hyperammonemia, could be the cause of hepatic encephalopathy (3). Hyperammonemia can induce disturbances in brain cell volume homeostasis (4), with an osmotically active intracellular accumulation of glutamine and counteraction of the resulting astrocyte swelling by *myo*-inositol depletion (3, 5). This situation is clearly reflected in ^{1}H-MRS in vivo studies of the brain of cirrhotic patients, which consistently show increases in the glutamine + glutamate signal accompanied by *myo*-inositol depletion (2, 4, 6–8). The osmoregulatory mechanism is activated after liver failure, and it accounts for the protection from massive brain edema in cases of chronic liver failure (9). Recent data suggest that clinical or minimal hepatic encephalopathy in cases of chronic liver disease may be the clinical manifestation of this low-grade astrocyte swelling (10, 11). However, signal abnormalities within the brain indicating cytotoxic edema have not been revealed by conventional MR imaging studies, probably because of their lack of sensitivity in detecting slight, diffuse, increased brain water content.

Unconventional MR imaging techniques, such as magnetization transfer imaging, are much more sensitive to changes in brain tissue water content, and these changes can be quantified through calculation of magnetization transfer ratios (MTR) (12). Previous studies showed MTR decreases in

Received October 16, 2000; accepted after revision January 15, 2001.

From the Magnetic Resonance Unit, Department of Radiology, Vall d'Hebron Teaching Hospitals, Barcelona, Spain.

This study was supported by a grant from Spain's Fondo de Investigación Sanitarias (Health Research Fund 98/231), awarded by the Ministry of Health and Welfare.

Address reprint requests to A. Rovira, Magnetic Resonance Unit (Department of Radiology), Hospital Universitari Vall d'Hebron, Passeig Vall d'Hebron 119-129, 08035 Barcelona, Spain.

the basal ganglia and cerebral white matter of patients with liver cirrhosis, although no attempt was made to establish correlations with the neurologic status of the patients or ^{1}H-MRS data (13, 14). Thus, the aim of this study was to determine, by means of MTR, whether there are significant changes in the brain parenchyma that evidence increases in free water and whether these changes correlate with ^{1}H-MRS abnormalities and the neurologic status of the patients.

Methods

Participants

A total of 24 patients (14 men and 10 women) with a mean age of 58 years (range, 30–68 years), referred from the Hepatology Department with a diagnosis of non-alcoholic cirrhosis, were prospectively enrolled in the study. The study was designed to exclude the confounding effects of alcohol on brain function and MR data (15). Eight healthy volunteers (two men and six women), with a mean age of 56.9 years, were also included. The study was approved by the Ethics Committee of our institution, and informed consent was obtained from each participant before being introduced in the protocol.

Diagnosis of cirrhosis was made on the basis of a consistent clinical history, radiologic studies, and liver biopsy, when available. The cause of cirrhosis was hepatitis C in 16 patients, hepatitis B in three, cryptogenetic in three, secondary biliary cirrhosis in one, and congenital alpha$_1$-antitrypsin deficiency in one. All patients showed evidence of portal hypertension and were being evaluated for liver transplantation because of liver failure (21 cases) or hepatocarcinoma (three cases). The severity of liver disease was staged according to the Child-Pugh classification; most cases were Child-Pugh class B (18 cases), and the remainder were class A (four cases) or C (two cases).

Neurologic and neuropsychological examinations were performed of all patients. The neuropsychological assessment consisted of a short battery of tests designed to provide a general evaluation of neuropsychological function and to detect the most frequently impaired functions. All participants were assessed by the same examiner by means of a structured interview that was completed in approximately 60 minutes, just before performing the MR imaging study. The neuropsychological evaluation included the following tests (16): Stroop Test, Trail Making Test (part A), Symbol Digits (oral version), Grooved Pegboard Test (dominant and non-dominant hand), Auditory Verbal Learning, Judgment of Line Orientation Hooper Test of Visual Organization, and Controlled Oral Word Association Test. Minimal hepatic encephalopathy was arbitrarily defined as two or more neuropsychological tests below 2 SD of the mean (17).

MR Examination and Analysis

The MR imaging studies were performed on a 1.5-T Magnetom Vision-Plus superconductive magnet (Siemens, Erlangen, Germany), using a quadrature transmit/receive head coil. Conventional MR imaging of the brain was performed initially and included the following pulse sequences: transverse T2-weighted fast spin-echo (3550/90 [TR/TE]; number of acquisitions, two) and T1-weighted inversion recovery spin-echo (1500/20; inversion time, 650 ms; number of acquisitions, one). A section thickness of 5 mm, an interleaved imaging mode with an intersection gap of 1.5 mm, a pixel size of approximately 1 × 1 mm, and an acquisition matrix of 256 × 256 were used to register the images. In addition, a magnetization transfer imaging study was performed in the transverse plane with a 2D gradient-echo pulse sequence (714/12; flip angle, 20 degrees; number of acquisitions, one), using the same section parameters and position as in the conventional sequences. The gradient-echo sequence was repeated with the same imaging parameters and an additional off-resonance preparation pulse used to saturate the macromolecular protons to obtain magnetization transfer contrast. This saturation pulse had the following parameters: off-resonance frequency selective gaussian RF pulse centered 1.5 kHz below the water frequency, bandwidth of 250 Hz, and length of 7.68 ms.

The conventional sequences were used to define the normal-appearing white matter regions in the frontal and parietal lobes. From a single T1-weighted image, we quantified the relative increased signal intensity of the globus pallidus through the globus pallidus index, a normalized signal measure of the globus pallidus compared with the putamen, by means of the following formula: globus pallidus signal – putamen signal/globus pallidus signal + putamen signal (Fig 1).

The MTR were quantified as a percentage of signal loss according to the following equation: MTR = 100 $(S_o - S_s)/S_{o,}$ in which S_o is the mean signal intensity for a particular region obtained from the 2D gradient-echo sequence without the saturation pulse and S_s is the mean signal intensity for the same region with the saturation pulse. Pixel-by-pixel MTR maps were constructed from the two sets of 2D gradient-echo images. To avoid misregistration between the two sets, a visual analysis that excluded mismatching of the MTR maps was conducted before calculating the MTR in selected areas. In case of mismatch, the two sets of images were repeated.

In both the patients and healthy volunteers, MTR of the normal-appearing white matter were measured in four different supratentorial locations, one in each of the frontal and parietal lobes of each hemisphere. The mean value of the MTR within selected areas was obtained by averaging the pixel values in the regions of interest on the MTR map (Fig 2).

Single-voxel proton spectra were obtained from a volume of interest located at the parietal region that was defined by a cube of 2 cm, containing mainly white matter (Fig 3). Voxel size was kept constant in all patients and control volunteers. A 90°–90°–90° stimulated-echo-based pulse sequence was used (18). Three chemical shift selective gaussian pulses were used for water suppression (19). Before recording the spectrum, the homogeneity of the magnetic field over the volume of interest was optimized by shimming on the water signal in two steps until a linewidth at half-height below 6 Hz was obtained. The first step was an automatic global shim and the second a manual shim with the three linear gradient coils over the selected voxel. After setting the water signal on resonance, the water suppression pulse was manually adjusted to reduce the water signal. Proton spectra were recorded with 1600/20 and a mixing time of 30 ms. A total of 1024 data points were collected over a spectral width of 1000 Hz. Four dummy images and 256 acquisitions were accumulated for each spectrum.

Spectrum analysis was performed off-line on a Silicon Graphics Indigo2 workstation (Silicon Graphics, Inc., Mountain View, CA) by means of the MRUI software, a graphical user interface for MR spectroscopy signal processing (20). The time domain data were analyzed with the AMARES method. This is a nonlinear least squares fitting that calculates the amplitude, which corresponds to the area of the resonance in the frequency domain, frequency, and linewidth at half-height of each signal. Before applying the AMARES method, the residual water signal was filtered with the Henkel-Lanczos singular value decomposition algorithm. Measurements were performed at the following resonances: *N*-acetyl aspartate (2.01 ppm), glutamine + glutamate (2.15−2.50 ppm), creatine + phosphocreatine (3.02 ppm), choline-containing compounds (3.20 ppm), and *myo*-inositol (3.55 ppm). Results are expressed as metabolite ratios with respect to the creatine + phosphocreatine resonance. The chemical shift for each resonance is referenced to the protons of the methyl group of the creatine signal at 3.02 ppm. Proton spectra and MTR analyses were

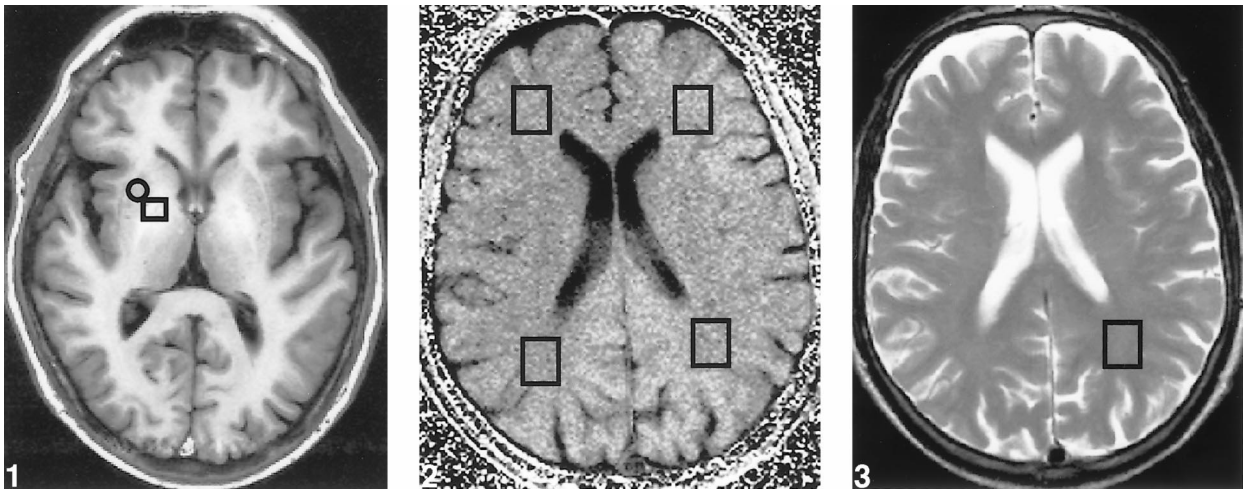

FIG 1. Transverse T1-weighted image (inversion recovery spin-echo; 1500/20; inversion time, 650 ms; number of acquisitions, one), obtained at the level of the basal ganglia in a patient with liver cirrhosis, shows bilateral increased signal in the globus pallidus. For calculating the globus pallidus index, mean signal intensity was calculated from a region of interest localized in both the putamen (□) and globus pallidus (○).

FIG 2. Transverse MTR map of a supraventricular level, obtained from two proton density gradient-echo sequences (714/12; flip angle, 20 degrees; number of acquisitions, one), the first with and the second without an off-resonance preparation pulse. MTR values were obtained from four different voxels (□) located in otherwise normal-appearing white matter, as defined on the T2-weighted sequence, within both parietal and frontal lobes.

FIG 3. Axial T2-weighted image (fast spin-echo; 3550/90; number of acquisitions, two), obtained at a supraventricular level, shows the voxel from which the ^{1}H-MRS image was obtained in the normal appearing white matter in the parietal lobe.

independently conducted by two observers blinded to the clinical condition of the participants.

Statistical Methods

Statistical analysis was conducted with the SPSS software package, version 7.5 (SPSS Inc., Chicago, IL). Significant differences were evaluated by means of the Student's *t* test or one-way analysis of variance. Pairwise comparisons were performed using Tukey's test. Correlations between MTR values and ^{1}H-MRS ratios were calculated using the Pearson's product-moment correlation coefficient. A P value $< .05$ was accepted as statistically significant for all the statistical analyses. Results are presented as mean ± SD.

Results

None of the patients showed signs of overt hepatic encephalopathy; all were perfectly alert, without flapping tremor, and were oriented in space, person, and time. However, according to the neuropsychological assessment, 16 of the patients were considered to have minimal hepatic encephalopathy.

All patients and healthy volunteers showed no significant white matter signal abnormalities on T2-weighted images, although increased signal intensity in the globus pallidus was observed on the T1-weighted images of all patients. Small focal or slightly diffuse high signal intensity abnormalities on the T2-weighted images, attributable to involutional changes or small vessel disease, were not considered to be significant white matter changes.

Mean MTR values of white matter in patients with liver cirrhosis were significantly lower than those of white matter in control volunteers, both in the parietal (31.5 ± 3.1 versus 37.1 ± 1.1; $P = .01$) and frontal (32.1 ± 3.4 versus 37.3 ± 1.7; $P = .01$) lobes (Table 1). MTR frontal and parietal white matter values were similar and closely correlated ($r = 0.88$; $P < .001$). No significant differences in MTR values were observed between cirrhotic patients with minimal hepatic encephalopathy and those without, although there was a tendency to higher MTR values in the patients without minimal hepatic encephalopathy (Table 2).

Globus pallidus indices were significantly higher in cirrhotic patients (0.145 ± 0.033) compared with healthy control volunteers (0.069 ± 0.007), but no significant differences were observed between the

TABLE 1: ^{1}H-MRS metabolite ratios from the parietal white matter, normalized globus pallidus intensity (GPI) and MTR of different brain regions for the control and cirrhotic groups.

	Control	Cirrhotic
N	8	21
Age	56.9 ± 3.6	57.8 ± 11.1
MTR parietal	37.1 ± 1.2	31.5 ± 3.1*
MTR frontal	37.3 ± 1.7	32.1 ± 3.4*
GPI	0.069 ± 0.007	0.145 ± 0.033*
NAA/Cr	1.57 ± 0.16	1.57 ± 0.18
NAA/Cho	2.02 ± 0.19	2.40 ± 0.47*
Cho/Cr	0.81 ± 0.11	0.68 ± 0.15*
Glx/Cr	1.46 ± 0.26	2.20 ± 0.48*
Ins/Cr	0.64 ± 0.10	0.28 ± 0.17*

Note.—All values are expressed as mean ± SD. Statistical significance was determined with a *t* test. A P value of less than .05 was used to assign significant difference.

* Significant difference between cirrhotic and control groups.

TABLE 2: ^{1}H-MRS metabolite ratios from the parietal white matter normalized globus pallidus intensity and MTR of different brain regions for cirrhotic patients classified by the existence of a minimal hepatic encephalopathy.

	Minimal Hepatic Encephalopathy	
	Yes	No
N	16	7
Age	57.8 ± 11.9	58.0 ± 9.6
MTR parietal	30.9 ± 3.4*	33.0 ± 1.6*
MTR frontal	31.6 ± 3.8*	33.4 ± 1.8*
GPI	0.144 ± 0.035*	0.148 ± 0.033*
NAA/Cr	1.57 ± 0.20	1.58 ± 0.13
NAA/Cho	2.42 ± 0.51	2.35 ± 0.39
Cho/Cr	0.67 ± 0.16*	0.69 ± 0.13*
Glx/Cr	2.37 ± 0.41*†	1.80 ± 0.39
Ins/Cr	0.22 ± 0.10*†	0.41 ± 0.23*

Note.—All values are expressed as mean ± SD. Statistical significance was determined with ANOVA followed by Tukey's test. A *P* value of less than .05 was considered statistically significant.

* Significant difference respect to the control group.

† Significant difference between patients with and without minimal hepatic encephalopathy.

patients with minimal hepatic encephalopathy (0.144 ± 0.035) and those without (0.148 ± 0.033).

Single-voxel ^{1}H-MRS of the parietal white matter showed the characteristic abnormalities that have been described in association with cirrhosis: decrease in the choline-containing compound:creatine + phosphocreatine ratio (0.68 ± 0.15 versus 0.81 ± 0.11; $P = .015$), decrease in the *myo*-inositol:creatine + phosphocreatine ratio (0.28 ± 0.17 versus 0.64 ± 0.10; $P < .01$), and increase in the glutamine + glutamate:creatine + phosphocreatine ratio (2.20 ± 0.48 versus 1.46 ± 0.26; $P < .01$) (Fig 4). There were no significant differences in *N*-acetylaspartate:creatine + phosphocreatine ratios between patients and control volunteers (1.57 ± 0.18 versus 1.57 ± 0.16) (Table 1).

The changes in *myo*-inositol:creatine + phosphocreatine and glutamine + glutamate:creatine + phosphocreatine ratios were significantly more decreased in cirrhotic patients with minimal hepatic encephalopathy than in those without minimal hepatic encephalopathy (0.22 ± 0.10 versus 0.41 ± 0.23 for *myo*-inositol:creatine + phosphocreatine

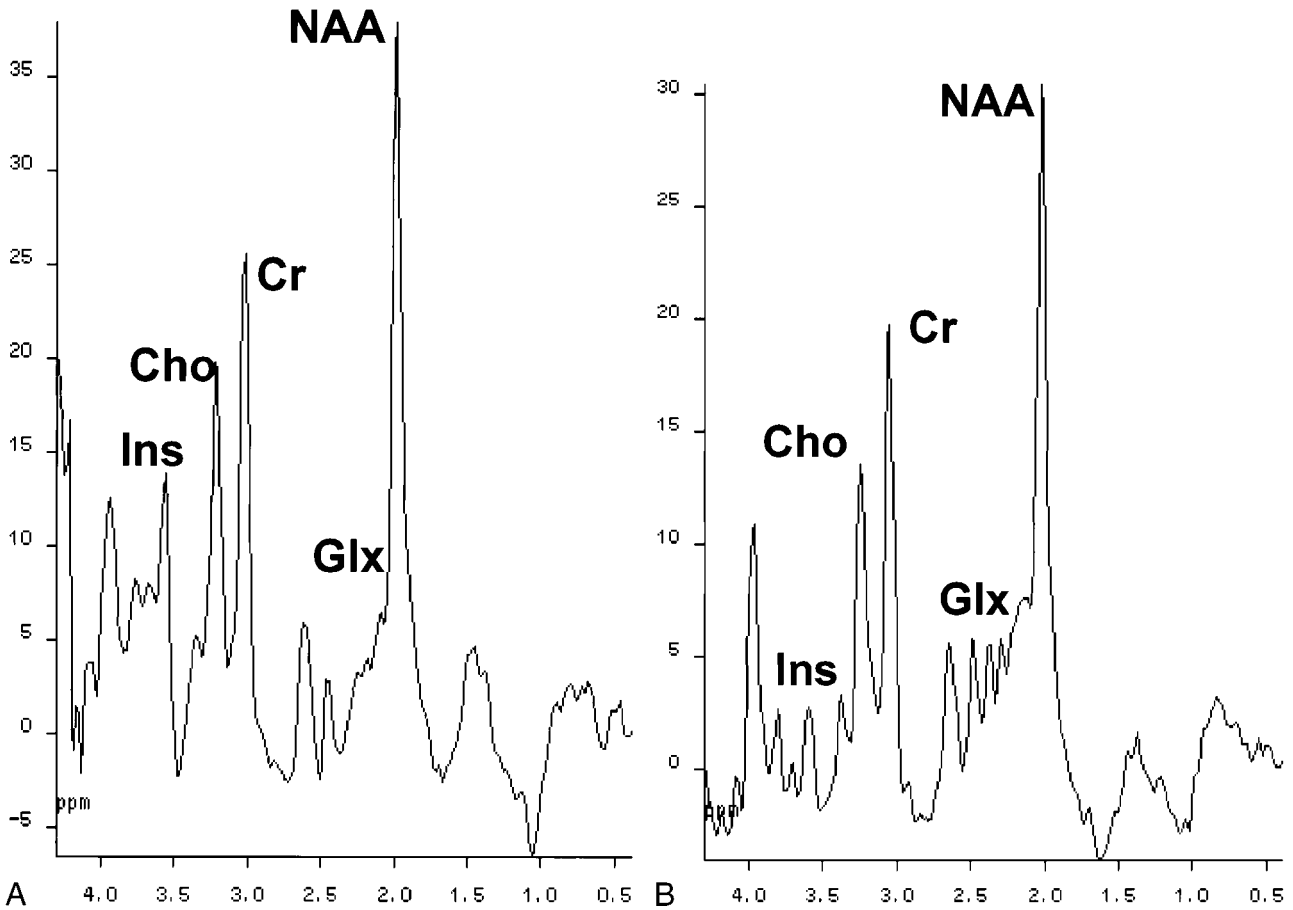

FIG 4. Water-suppressed proton spectra of an 8-mL voxel located in the parietal region, recorded with a stimulated echo-based pulse sequence (1600/20; magnetization transfer, 30; number of acquisitions, 256). The main resonances correspond to *N*-acetylaspartate (2.0 ppm), glutamic/glutamine (2.1–2.5 ppm), creatine/phosphocreatine (3.02 ppm), choline-containing compounds (3.2 ppm), and *myo*-inositol (3.55 ppm). Comparison of the spectra shows a decrease in choline and *myo*-inositol resonances, with an increase in the glutamic/glutamine region in the cirrhotic patient.

A, Healthy control volunteer.

B, Cirrhotic patient.

and 2.37 ± 0.41 versus 1.80 ± 0.39 for glutamine + glutamate:creatine + phosphocreatine) (Table 2). A significant correlation was observed between MTR values and glutamine + glutamate:creatine + phosphocreatine ratios ($r = -0.65$; $P = .002$) and the globus pallidus index ($r = -0.61$; $P = .002$) in patients with liver cirrhosis.

Discussion

Magnetization transfer imaging represents an attempt to develop contrast in MR imaging on the basis of submolecular exchange processes that may occur in biological tissue (21). This technique has some clinical and research applications in the study of different CNS disorders (22), because it affords a potential window into the macromolecular environment that is not directly visible using conventional techniques (21). Therefore, it enables the assessment of ''invisible'' disease in the so-called *normal-appearing white matter* (23–25), and, with the application of MTR, it provides a means to quantify disease burden (26).

Experimental and human studies support the hypothesis that demyelination and axonal loss are the main contributors to the MTR decrease observed in association with several pathologic conditions, such as experimental autoimmune encephalomyelitis (12), toxic demyelination (27), progressive multifocal leukoencephalopathy (28), human immunodeficiency virus encephalitis (28), and multiple sclerosis (29). Severe MTR decrease correlates directly with the severity of demyelination and axonal loss, but less severe decrease is more difficult to interpret because inflammation, edema, and moderate demyelination can also contribute to these values (30).

Purely edematous lesions may decrease MTR values slightly, although significantly. This suggestion is based on data obtained in experimental models of edematous inflammatory non-demyelinated lesions of the CNS (12) and in cases of chronic obstructive hydrocephalus (31).

MTR decreases in otherwise normal-appearing cerebral white matter have been described previously in association with liver cirrhosis (13). However, for the first time, we correlate this change with the patients' neurologic status and with ^{1}H-MRS abnormalities. The still unproven mechanism of MTR decrease reflects a diffuse tissue abnormality not detectable by conventional MR imaging. Previous data have suggested that this reduction may be produced by low-grade astrocyte swelling, the main pathophysiological event related to clinical or minimal hepatic encephalopathy (10, 11). The astrocyte swelling may be due to an osmotically active intracellular accumulation of glutamine in response to hyperammonemia; this situation then activates an osmoregulatory mechanism with decreases of intracellular *myo*-inositol that protects the brain from massive edema (10). This disturbance of cell volume homeostasis is clearly reflected in the pattern of ^{1}H-MRS changes observed in cases of cirrhosis (2).

Other possible contributions to the decrease of MTR are unlikely. Although it has been found that manganese chloride phantoms reduce MTR values and that MTR of the pallidus decreases with the severity of liver disease (14), the presence of manganese deposits in the white matter as the origin of MTR reduction is improbable, because there is no concomitant T1 shortening of the white matter. Slight axonal loss or demyelination are also unlikely explanations for the MTR decrease in cases of cirrhosis. These pathologic features have not been described in association with liver encephalopathy, and moreover, the ^{1}H-MRS findings of normal *N*-acetylaspartate indices and low concentrations of choline-containing compounds indicate preservation of axonal density and lack of demyelinating processes.

Thus, the most likely explanation for the slight, although significant, decrease in MTR values in normal-appearing white matter of cirrhotic patients is low-grade astrocyte swelling. The application of diffusion-weighted MR imaging studies, a highly sensitive technique for detecting water shifts between the intra- and extracellular spaces (32, 33), would determine whether the increased brain water content came from the intracellular or extracellular compartment. Unfortunately, at the time we started the study, diffusion-weighted sequences could not be performed with our unit.

However, if we accept the hypothesis that low grade intracellular swelling is the leading event in the pathogenesis of liver encephalopathy (11), our results should show a significant difference in the MTR between patients having minimal hepatic encephalopathy and those without minimal hepatic encephalopathy, as was found with glutamine + glutamate and *myo*-inositol ratios and subclinical altered mental states. These contradictory results may be explained by the lower sensitivity of MTR as compared with ^{1}H-MRS for detecting white matter abnormalities induced by the osmoregulatory stress in patients with chronic liver disease but without overt hepatic encephalopathy. MTR assessment in cirrhotic patients with overt hepatic encephalopathy would probably show a significant decrease in the MTR as compared with patients with minimal or no hepatic encephalopathy. Thus, our data suggest that MTR cannot be used as a marker of subclinical encephalopathy in patients with chronic liver disease but might play a role as a surrogate marker in longitudinal studies designed for assessing the effect of therapy in clinical or subclinical hepatic encephalopathy.

The significant correlation between the globus pallidus index and MTR decrease can be interpreted as two different MR changes induced by chronic liver disease having completely different pathogenic mechanisms: increased whole blood manganese concentrations for the increase in globus pallidus index (34, 35) and disturbed cell volume homeo-

stasis in response to hyperammonemia for the decreased MTR.

Conclusion

Patients with liver cirrhosis had significantly decreased MTR values of the brain white matter, which correlated with an increase in brain glutamine + glutamate. The MTR decrease can be explained by disturbed cerebral cell volume homeostasis causing an increase in the volume of the free water compartment that leads to astrocyte swelling. Although this low-grade intracellular swelling is considered to be the main contributor to hepatic encephalopathy, we could not show a significant correlation between MTR decrease and presence of minimal hepatic encephalopathy. This can be explained by the small number of patients included in the study and by limitations in the sensitivity of MTR for detecting low-grade intracellular edema.

Longitudinal MR imaging studies that include diffusion-weighted sequences, performed after normalization of liver function and improvement in neurologic status, might provide evidence to support the hypothesis that MTR decrease reflects potentially reversible low-grade intracellular edema. Such studies would add to our knowledge of the pathophysiology of liver encephalopathy and define the potential use of MR imaging as a surrogate marker for assessing therapy in clinical or minimal hepatic encephalopathy in chronic liver disease.

Acknowledgment

The authors thank Celine L. Cavallo for editing the manuscript.

References

1. Kulisevsky J, Pujol J, Balanzó J, et al. **Pallidal hyperintensity on magnetic resonance imaging in cirrhotic patients: clinical correlations.** *Hepatology* 1992;16:1382–1388
2. Ross BD, Jacobson S, Villamil F, et al. **Subclinical hepatic encephalopathy: proton MR spectroscopic abnormalities.** *Radiology* 1994;193:457–463
3. Butterworth RF, Giguere JF, Michaud J, Lavoie J, Layrargue GP. **Ammonia: key factor in the pathogenesis of hepatic encephalopathy.** *Neurochem Pathol* 1987;6:1–12
4. Häusinger D, Laubenberger J, vom Dahl S, et al. **Proton magnetic resonance spectroscopic studies on human brain myo-inositol in hypo-osmolarity and hepatic encephalopathy.** *Gastroenterology* 1994;107:1475–1480
5. Basile AS, Jones EA. **Ammonia and GABA-ergic neurotransmission: interrelated factors in the pathogenesis of hepatic encephalopathy.** *Hepatology* 1997;25:1303–1305
6. Lee JH, Seo DW, Lee YS, et al. **Proton magnetic resonance spectroscopy (^{1}H-MRS) findings for the brain in patients with liver cirrhosis reflect the hepatic functional reserve.** *Am J Gastroenterol* 1999;94:2206–2213
7. Laubenberger J, Häusinger D, Bayer S, Gufler H, Henning J, Langer M. **Proton magnetic resonance spectroscopy of the brain in symptomatic and asymptomatic patients with liver cirrhosis.** *Gastroenterology* 1997;112:1610–1616
8. Geissler A, Lock G, Fründ R, et al. **Cerebral abnormalities in patients with cirrhosis detected by proton magnetic resonance spectroscopy and magnetic resonance imaging.** *Hepatology* 1997;25:48–54
9. Córdoba J, Gottstein J, Blei AT. **Glutamine, myo-inositol, and organic brain osmolytes after portocaval anastomosis in the rat: implications for ammonia-induced brain edema.** *Hepatology* 1996;24:919–923
10. Córdoba J, Blei AT. **Brain edema and hepatic encephalopathy.** *Semin Liver Dis* 1996;16:271–280
11. Häussinger D, Kircheis G, Fischer R, Schliess F, vom Dahl S. **Hepatic encephalopathy in chronic liver disease: a clinical manifestation of astrocyte swelling and low-grade cerebral edema?** *J Hepatol* 2000;32:1035–1038
12. Dousset V, Grossman RI, Ramer KN, et al. **Experimental allergic encephalomyelitis and multiple sclerosis: lesion characterization with magnetization transfer imaging.** *Radiology* 1992;182:483–491
13. Iwasa M, Kinosada Y, Natatsuka A, Watanabe S, Adachi Y. **Magnetization transfer contrast of various regions of the brain in liver cirrhosis.** *AJNR Am J Neuroradiol* 1999;20:652–654
14. Iwasa M, Kinosada Y, Watanabe S, et al. **Hepatic cirrhosis: magnetization transfer contrast in globus pallidus.** *Neuroradiology* 1998;40:145–149
15. Seitz D, Widmann U, Seeger U, et al. **Localized proton magnetic resonance spectroscopy of the cerebellum in detoxifying alcoholics.** *Alcohol Clin Exp Res* 1999;23:158–163
16. Blei AT, Córdoba J. **Subclinical encephalopathy.** *Dig Dis* 1996;14[suppl 1]:2–11
17. Lezak MD. ***Neuropsychological Assessment.*** 3rd ed. Oxford: Oxford University Press; 1995
18. Frahm J, Merboldt KD, Hänicke W. **Localized proton spectroscopy using stimulated echoes.** *J Magn Reson* 1987;72:502–508
19. Haase A, Frahm J, Hänicke W, Matthaei D. **^{1}H NMR chemical shift selective (CHESS) imaging.** *Phys Med Biol* 1985;30:341–344
20. van den Boogaart A, Vanhamme L. ***MRUI Manual Version 96.3: A User's Guide to the Magnetic Resonance User Interface Software Package.*** Delft: Delft Technische Universiteit Press; 1997
21. Wolff SD, Balaban RS. **Magnetization transfer imaging: practical aspects and clinical applications.** *Radiology* 1994;192:593–599
22. van Buchem MA. **Magnetization transfer: applications in neuroradiology.** *J Comput Assist Tomogr* 1999;23[suppl 1]:S9–S18
23. Filippi M, Campi A, Dousset V, et al. **A magnetization transfer imaging study of normal-appearing white matter in multiple sclerosis.** *Neurology* 1995;45:478–482
24. Loevner LA, Grossman RI, Cohen JA, Lexa FJ, Kessler D, Kolson DL. **Microscopic disease in normal-appearing white matter on conventional MR imaging in patients with multiple sclerosis: assessment with magnetization-transfer measurements.** *Radiology* 1995;196:511–515
25. Hiehle JF, Lenkinski RE, Grossman RJ, et al. **Correlation of spectroscopy and magnetization transfer imaging in the evaluation of demyelinating lesions and normal appearing white matter in multiple sclerosis.** *Magn Reson Med* 1994;32:285–293
26. Filippi M, Rovaris M. **Magnetisation transfer imaging in multiple sclerosis.** *J Neurovirol* 2000;6[suppl 2]:S115–S120
27. Dousset V, Brochet B, Vital A, et al. **Lysolecithin-induced demyelination in primates: preliminary in vivo study with MR and magnetization transfer.** *AJNR Am J Neuroradiol* 1995;16:225–231
28. Dousset V, Armand JP, Lacoste D, et al. **Magnetization transfer study of HIV encephalitis and progressive multifocal leukoencephalopathy.** *AJNR Am J Neuroradiol* 1997;18:895–901
29. van Waesberghe JH, Kamphorst W, van Walderveen MA, et al. **Histopathologic correlate of MTR and hypointense signal intensity on T1 SE in multiple sclerosis: a direct postmortem study.** *Multiple Sclerosis* 1998;4:272
30. Brochet B, Dousset V. **Pathological correlates of magnetization transfer imaging abnormalities in animal models and humans with multiple sclerosis.** *Neurology* 1999;53[suppl 3]:12–17
31. Hähnel S, Münkel K, Jansen O, et al. **Magnetization transfer measurements in normal-appearing cerebral white matter in patients with chronic obstructive hydrocephalus.** *J Comput Assist Tomogr* 1999;23:516–520
32. Latour L, Svoboda K, Mitra P. **Time dependent diffusion of water in a biological model system.** *Proc Natl Acad Sci U S A* 1994;91:1229–1233
33. van der Toorn A, Sykova E, Dijkhuizen RM, et al. **Dynamic changes in water ADC, energy metabolism, extracellular space volume, and tortuosity in neonatal rat brain during global ischemia.** *Magn Reson Med* 1996;36:52–60
34. Krieger D, Krieger S, Jansen O, Gass P, Theilmann L, Lichtnecker H. **Manganese and chronic hepatic encephalopathy.** *Lancet* 1995;346:270–274
35. Rose C, Butterworth RF, Zayed J, et al. **Manganese deposition in basal ganglia structures results from both portal-systemic shunting and liver dysfunction.** *Gastroenterology* 1999;117:640–644